APPENDIX A

COMPUTER FILES LISTING

Geometry Inputs (Geometry_Inputs.zip) [1]	Description
HL_Drain_MISO.INP	Main geometry input file that uses all the files listed below
MProp_MISO_PALS.INP [2]	Revised material property input file
Deg90_lines.INP	Sub-Geometry file that is used in the main file - HL_Drain_*.INP
Deg120_lines.INP	Sub-Geometry file that is used in the main file - HL_Drain_*.INP
Deg150_lines.INP	Sub-Geometry file that is used in the main file - HL_Drain_*.INP
Deg180_lines.INP	Sub-Geometry file that is used in the main file - HL_Drain_*.INP
first30vol.INP	Sub-Geometry file that is used in the main file - HL_Drain_*.INP
second30vol.INP	Sub-Geometry file that is used in the main file - HL_Drain_*.INP
third30vol.INP	Sub-Geometry file that is used in the main file - HL_Drain_*.INP
IDpatch_volmesh.INP	Sub-Geometry file that is used in the main file - HL_Drain_*.INP
weldmesh.INP	Sub-Geometry file that is used in the main file - HL_Drain_*.INP
IDpatch_fix.INP	Sub-Geometry file that is used in the main file - HL_Drain_*.INP
butterlike_volmesh.INP	Sub-Geometry file that is used in the main file - HL_Drain_*.INP
cladnextto_IDpatch.INP	Sub-Geometry file that is used in the main file - HL_Drain_*.INP
volnextto_butterlike.INP	Sub-Geometry file that is used in the main file - HL_Drain_*.INP
boss.INP	Sub-Geometry file that is used in the main file - HL_Drain_*.INP
pipeandclad.INP	Sub-Geometry file that is used in the main file - HL_Drain_*.INP
HL_Drain_COMPONENTS1.INP	Sub-Geometry file that is used in the main file - HL_Drain_*.INP
clearfornewscheme.INP	Sub-Geometry file that is used in the main file - HL_Drain_*.INP
autoweld.INP	Sub-Geometry file that is used in the main file - HL_Drain_*.INP
movetheboss.INP	Sub-Geometry file that is used in the main file - HL_Drain_*.INP
selection.INP	Sub-Geometry file that is used in the main file - HL_Drain_*.INP
newnugidpatch.INP	Sub-Geometry file that is used in the main file - HL_Drain_*.INP
selbutter.INP	Sub-Geometry file that is used in the main file - HL_Drain_*.INP
workontheboss.INP	Sub-Geometry file that is used in the main file - HL_Drain_*.INP
newpipeandcladparts.INP	Sub-Geometry file that is used in the main file - HL_Drain_*.INP
HL_Drain_COMPONENTS2.INP	Sub-Geometry file that is used in the main file - HL_Drain_*.INP

Notes:
1. All files with the exception of MProp_MISO_PALS.INP are obtained from [1]
2. This file contains the updated material properties, as listed in Tables 1 through 8.

Residual Stress Files (Residual_Files.zip)	Description
BCNUGGET3D.INP	Weld pass and model boundary definition file
THERMAL3D.INP	Input file to perform the thermal pass of welding simulation
THM_PWHT.INP	Input file to perform the thermal pass of PWHT
STRESS3D.INP	Input file to perform the stress pass of welding simulation
CBC.INP	Input file to apply mechanical boundary conditions and creep properties. Read in STRESS3D.INP
THM_PWHT_mntr.inp	Processed thermal pass load steps for PWHT. Read in STRESS3D.INP
INSERT3D.INP	Input file to perform the stress pass of hydrostatic test and 5 NOC cycles. Read in STRESS3D.INP
WELD#_mntr.inp	Processed thermal pass load steps for stress pass. # = 1-3
*.mac	WRS analysis macro files required for analysis
THERMAL3D.TXT	Parameter input file for thermal pass of welding simulation
STRESS3D.TXT	Parameter input file for stress pass
POST_AXIAL.INP	Post-processing input file to extract hoop stress for axial cracks
Hoop_0.csv	Formatted hoop stress outputs for axial cracks
GETPATH.TXT	Stress path (P1& P2) definitions for investigating PWHT thru-wall stresses

Circ Crack Files (Circ_Crack_Files.zip)	Description
FM_STACK.INP	Controller input file LEFM analysis files execution sequence
Crack#.INP	Geometry input files to create circ. crack at specified depth. # = 0-6 With 0 = 0.13", 1 = 0.57", 2 = 1.12", 3 = 1.85", 4 = 2.49", 5 = 3.13", 6 = 3.95"
Crack_nodes#.inp	Crack tip node inputs for fracture mechanics model conversion. # = 0-6
AnTip80.mac	Macro to insert crack tip elements to the fracture mechanics model and extract K results
Crack#_COORD.INP	Input files to determine crack face element centroid coordinates. # = 0-6
Crack#_COORD1.txt	Crack face element centroid coordinate outputs. # = 0-6
Crack#_GETSTR.INP	Input files to extract crack face stresses from residual stress analysis. # = 0-6
STR_FieldOper_#1.txt	Extracted crack face stresses from residual stress analysis. # = 0-6
Crack#_IMPORT.INP	Input files to transfer stresses into crack face pressure (plus operating pressure on crack face) and solve for solution. # = 0-6
AnTip80_KCALC.INP	KCALC post-processing input file
Crack#_IMPORT_K.CSV	Formatted K result outputs. # = 0-6
1200895.306r1.xlsx	Excel spreadsheet containing creep data, PWHT comparison, and K results
1200895.306r1.pptx	PowerPoint slides of selected figures and result plots

Structural Integrity Associates, Inc.®	File No.: 1200895.307
CALCULATION PACKAGE	**Project No.: 1400148** Quality Program: ☒ Nuclear ☐ Commercial

PROJECT NAME:
Evaluation of Hot Leg Drain Nozzle

CONTRACT NO.:
10404220

CLIENT:	**PLANT:**
Entergy Nuclear	Palisades Nuclear Plant

CALCULATION TITLE:
Hot Leg Drain Nozzle Crack Growth Analyses

Document Revision	Affected Pages	Revision Description	Project Manager Approval Signature & Date	Preparer(s) & Checker(s) Signatures & Date
0	1 - 12	Initial Issue	Richard Bax 03/06/14	Dilip Dedhia 03/06/14 Charles Fourcade 03/06/14
1	1 - 12	Recalculated remaining life to incorporate new stresses for axial cracks and new Ks for circumferential cracks.	Norman Eng NE 5/8/15	Preparer: Dilip Dedhia Dilip Dedhia DDD 5/8/15 Checkers: Minji Fong Minji Fong MF 5/8/15 Stan Tang SST 5/8/15

Table of Contents

List of Tables

List of Figures

1.0 OBJECTIVE

The objective of this calculation is to determine crack growth for a series of postulated cracks in the hot leg to drain nozzle boss weld in support of a Primary Water Stress Corrosion Cracking (PWSCC) susceptibility study at the Palisades Nuclear Plant (PNPP). The PWSCC crack growth analyses are performed using extracted stresses and stress intensity factors for both circumferential and axial cracks. All the files used in this calculation are listed in Table 1.

Revision 1 corrects an error in the pressure application for the hydrostatic test and normal operating cycle load steps.

2.0 METHODOLOGY

PWSCC crack growth analyses are performed for circumferential and axial cracks in the hot leg to drain nozzle boss weld.

2.1 Crack Growth Rate

The default PWSCC crack growth rate in **pc-CRACK** [1] will be employed. This relation is based on expressions in Reference 2 and the resulting equation for the crack growth rate is as follows:

$$\frac{da}{dt} = C\exp\left[-Q\left(\frac{1}{T+460}-\frac{1}{T_{ref}+460}\right)\right](K-K_{th})^{\beta} \quad (1)$$

For times in hours, temperatures in °F, crack length in inches and K in ksi-√in, the following values of the constants are used:

T_{ref} = 617°F
C = 2.47x10^{-7}
β = 1.6
Q = 28181.8°R
K_{th} = 0

2.2 Circumferential Cracks

Stress intensity factors (K) for a series of 360° inside surface connected, part through wall (0.13", 0.57", 1.21", 1.85", 2.49", 3.13", and 3.95") circumferential cracks were calculated using finite element analysis (FEA) in Table 10 of Reference 3. These K values, as a function of crack depth, were extracted at 0, 30, 60 and 90 degree locations around the nozzle and are shown in Figure 1. These K values were input into **pc-CRACK** to perform PWSCC crack growth analyses. The following are the additional parameters needed for the crack growth calculations:

Initial crack depth = 0.1"
Temperature = 593°F (operating temperature per Reference 4)

Wall thickness = 4.08" (the height of the weld, per Reference 3)

The initial crack size is based on expected engineering flaw sizes that could be present for a crack that would then grow by PWSCC. The final flaw size for these analyses is 75% of the wall thickness. This final depth is chosen as it is the maximum allowable flaw depth per ASME Code Section XI, IWB-3643 [6]. The resulting crack depths, as a function of time, as calculated by **pc-CRACK** are shown in Figure 2. The input and the output files are tabulated in Table 1.

The crack depths for 20, 30, 40, 50 and 60 years of crack growth are listed in Table 2 at a series of angular locations.

2.3 Axial Cracks

The hoop stresses (relative to the drain nozzle) at the weld and nozzle region are extracted from the stresses computed by FEA [3]. The rectangular region under consideration for the location of axial cracks (axial in this case indicating a nozzle radial crack aligned in the axial direction of the hot leg) is shown in Figure 3. The crack model of interest is a semi-elliptical crack with a fixed surface length and the depth varying from 0.1" to 3.5". Since there is no stress intensity factor influence function solution available in **pc-CRACK** for semi-elliptical surface cracks for the range of crack shapes with bivariate stresses, the influence function solution for an elliptical crack available in ***SmartCrack*** [5] was used. Half of the elliptical crack was placed in the region as shown in Figure 4. The stresses on the other half of the ellipse, needed for computing stress intensity factors, were defined by reflecting the stresses across the ID of the hot leg, as shown in Figure 4. The cracked body can be sliced at this plane, with a semi-elliptical surface crack then being present. The methodology to compute the stress intensity factors can be considered as the best approximation for the problem. The crack face pressure of 2.122 ksi (operating pressure from Reference 4) was added to the FEA calculated stresses.

A new coordinate system is defined for inputting stresses into ***SmartCrack***. The new X-coordinate is along the hot leg ID, except that the origin is at the center of the crack. The new Y-coordinate is along the weld depth with the origin at the center of the crack. The stresses in the new coordinate system are developed in *Hoop_2015.xlsm*.

SmartCrack requires stresses along the X-direction to be defined for each depth (y). The stresses from *Hoop_2015.xlsm* are reformatted and three ***SmartCrack*** input files are created corresponding to the total surface length of 0.5", 1" and 2", respectively. These files also contain the definition of the crack model. These files were then run with ***SmartCrack*** and the output is listed in *H00-2-1.OUT*, *H00-2-2.OUT* and *H00-2-3.OUT*, corresponding to the total surface length of 0.5", 1" and 2", respectively. The output files contain the echo of the input stresses and the stress intensity factors at the four tips of the elliptical crack for a range of crack sizes. The crack tip of interest is a3 in the ***SmartCrack*** output. The K values (see Figure 5) corresponding to the crack tip a3 were extracted for use in PWSCC crack growth evaluations using **pc-CRACK**. The following are the additional parameters needed for the crack growth calculations:

Initial crack depth = 0.1"
Temperature = 593°F (operating temperature per Reference 4)
Wall thickness = 4.0" (the height of the weld, per Reference 3)

The initial crack size is based on expected engineering flaw sizes that could be present for a crack that would then grow by PWSCC. The final flaw size for these analyses is 75% of the wall thickness. This final depth is chosen as it is the maximum allowable flaw depth per ASME Code Section XI, IWB-3643 [6]. Additional sensitivity analyses are also performed as described later in this section.

A review of Figure 6 indicates that the time to grow the crack from 0.1" to 3" (75% through wall) is 17.7 years for the case of 1" total surface length and 11.3 years for 2" total surface length. For the case of the 0.5" total surface length, the crack has not yet reached 3" after approximately 60.2 years.

Additional crack growth results were generated by changing the initial crack size to 0.025", temperature to 580°F and 583°F and by adding 5 ksi tensile stress to the base case (H00-2-3.DAT). The total surface length of the crack was 2". The time to grow the crack from 0.025" to both 75% and 93.125% of the wall are reported in Table 2. Since the calculated stress intensity factors only extended up to a crack size of 3.5", it was assumed that the stress intensity factors beyond 3.5" were the same as at 3.5". This is considered a conservative assumption since the stress intensity valued are decreasing in that region. This assumption allows the calculation of life for cracks growing all the way to 93.125% of the wall.

3.0 CONCLUSIONS

Stress intensity factors, K, for various 360° part through-wall circumferential flaws in the hot leg drain nozzle-to-hot leg weld, resulting from weld residual stresses, were evaluated to determine circumferential flaw growth due to PWSCC. The results of these evaluations are tabulated in Table 3 and shown in Figure 2.

In addition, hoop stresses in the hot leg drain nozzle-to-hot leg weld and adjacent nozzle, resulting from weld residual stresses, were also evaluated to determine the axial flaw growth due to PWSCC. The results of these evaluations are shown in Figure 6.

4.0 REFERENCES

1. **pc-CRACK 4.1,** Version 4.1 CS, Structural Integrity Associates, December 2013.

2. SI Calculation No. 0801136.315, Rev. 0, "Hot Leg Drain Crack Growth Projections."

3. SI Calculation No. 1200895.306, Rev. 1, "Hot Leg Drain Nozzle Weld Residual Stress Analysis and Circumferential Crack Stress Intensity Factor Determination."

4. Palisades Document No. EC-LATER, Revision 0, "Design Input Record," SI File No. 0801136.202.

5. SI Calculation No. 0801136.313, Rev. 0, "Hot Leg Nozzles Methodology for Development of Stress Intensity Factor."

6. ASME Boiler and Pressure Vessel Code, Section XI, 2001 Edition with Addenda through 2003.

Table 1: List of Files

File	Description
CircCrackDeg 00.pcf	**pc-CRACK** PWSCC growth input file; K at 0 deg
CircCrackDeg 30.pcf	**pc-CRACK** PWSCC growth input file; K at 30 deg
CircCrackDeg 60.pcf	**pc-CRACK** PWSCC growth input file; K at 60 deg
CircCrackDeg 90.pcf	**pc-CRACK** PWSCC growth input file; K at 90 deg
CircCrackDeg 00.rpt	**pc-CRACK** PWSCC growth output file; K at 0 deg
CircCrackDeg 30.rpt	**pc-CRACK** PWSCC growth output file; K at 30 deg
CircCrackDeg 60.rpt	**pc-CRACK** PWSCC growth output file; K at 60 deg
CircCrackDeg 90.rpt	**pc-CRACK** PWSCC growth output file; K at 90 deg
Hoop_2015.xlsm	FEA calculated stresses for axial cracks from Reference [3]
H00-2-1.DAT	***SmartCrack*** K input file for crack surface length = 0.5"
H00-2-2.DAT	***SmartCrack*** K input file for crack surface length = 1"
H00-2-3.DAT	***SmartCrack*** K input file for crack surface length = 2"
H00-2-1.OUT	***SmartCrack*** K output file for crack surface length = 0.5"
H00-2-2.OUT	***SmartCrack*** K output file for crack surface length = 1"
H00-2-3.OUT	***SmartCrack*** K output file for crack surface length = 2"
Hoop-1.pcf	**pc-CRACK** PWSCC growth input file for crack surface length = 0.5"
Hoop-2.pcf	**pc-CRACK** PWSCC growth input file for crack surface length = 1"
Hoop-3.pcf	**pc-CRACK** PWSCC growth input file for crack surface length = 2"
Hoop-1.rpt	**pc-CRACK** PWSCC growth output file for crack surface length = 0.5"
Hoop-2.rpt	**pc-CRACK** PWSCC growth output file for crack surface length = 1"
Hoop-3.rpt	**pc-CRACK** PWSCC growth output file for crack surface length = 2"
SC-P0.DAT	***SmartCrack*** K input file for Original Stress (same as H00-2-3.DAT)
SC-P5.DAT	***SmartCrack*** K input file for Original Stress + 5 ksi
SC-P0.OUT	***SmartCrack*** K output file for Original Stress
SC-P5.OUT	***SmartCrack*** K output file for Original Stress + 5 ksi
Hoop-P0-580.pcf	**pc-CRACK** PWSCC growth input file for Original Stress, 580°F, 0.025" initial crack size
Hoop-P0-580.rpt	**pc-CRACK** PWSCC growth output file for Original Stress, 580°F, 0.025" initial crack size
Hoop-P5-580.pcf	**pc-CRACK** PWSCC growth input file for Original Stress + 5 ksi, 580°F, 0.025" initial crack size
Hoop-P5-580.rpt	**pc-CRACK** PWSCC growth output file for Original Stress + 5 ksi, 580°F, 0.025" initial crack size
Hoop-P0-583.pcf	**pc-CRACK** PWSCC growth input file for Original Stress, 583°F, 0.025" initial crack size
Hoop-P0-583.rpt	**pc-CRACK** PWSCC growth output file for Original Stress, 583°F, 0.025" initial crack size
Hoop-P5-583.pcf	**pc-CRACK** PWSCC growth input file for Original Stress + 5 ksi, 583°F, 0.025" initial crack size
Hoop-P5-583.rpt	**pc-CRACK** PWSCC growth output file for Original Stress + 5 ksi, 583°F, 0.025" initial crack size

Table 2: Additional Crack Growth Evaluations for Axial Crack

Run #	Stress Field	Initial Flaw Depth (inches)	Temperature (°F)	Time (years) for crack to grow to a given depth	
				75%	93.125%
0[(1)]	Original	0.1"	593	11.3	--
1	Original	0.025"	580	16.9	22.3
2	Original	0.025"	583	15.6	20.7
3	Original + 5 ksi	0.025"	580	12.8	16.6
4	Original + 5 ksi	0.025"	583	11.8	15.4

Note: (1) Base case, H00-2-3.DAT, surface length of the crack = 2"

Table 3: Crack Depths at 20-60 years for the Circumferential Cracks

Angular Location (degrees)[(1)]	Crack Depth (inches)				
	20 years	30 years	40 years	50 years	60 years
0	2.07	2.50	2.83	3.04	3.20
30	2.25	2.78	3.11	3.61	TW
60	2.74	3.51	TW	TW	TW
90	3.05	TW	TW	TW	TW

Note: (1) Angular locations are based on the finite element model shown in Figure 1 of Reference 3.

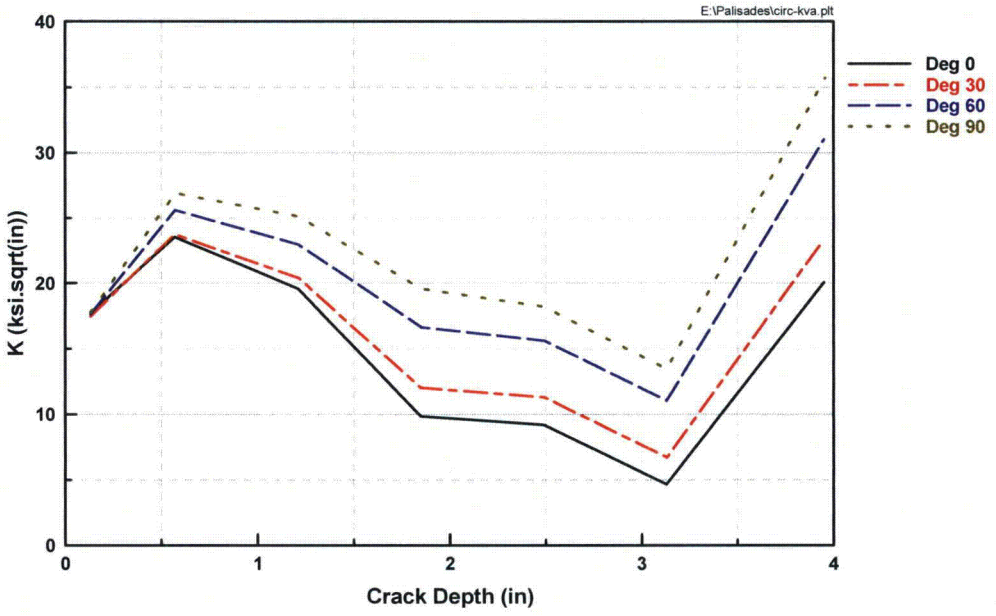

Figure 1: FEA Calculated Stress Intensity Factors for Circumferential Cracks

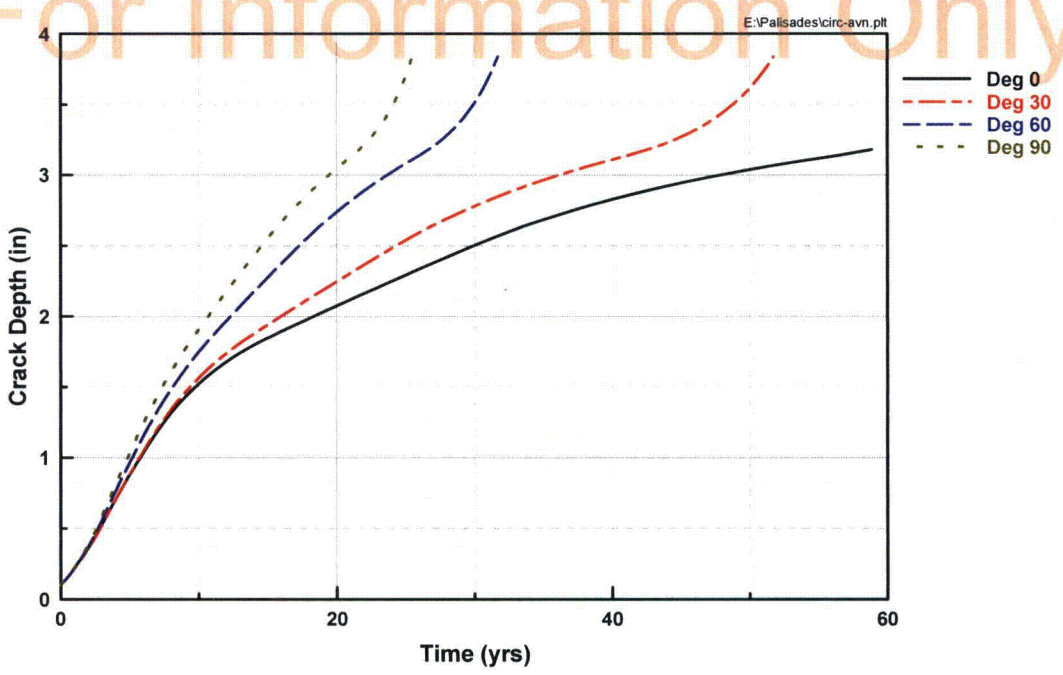

Figure 2: Crack Depth vs. Time for the Growth of Circumferential Cracks

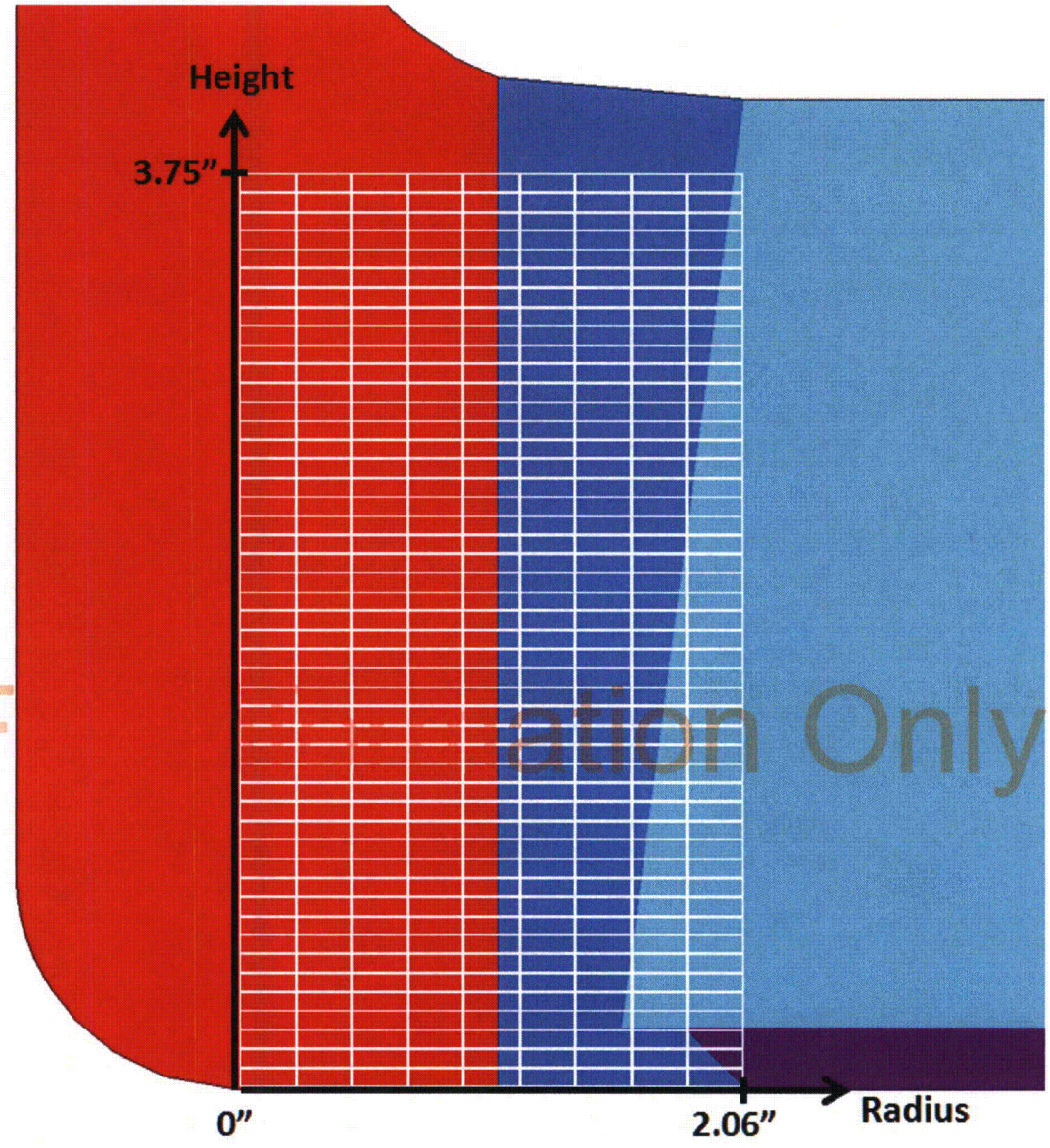

Figure 3: Plane on which the Axial Cracks are Located

Note:
1. Figure is reproduced from Reference 3, Figure 20.

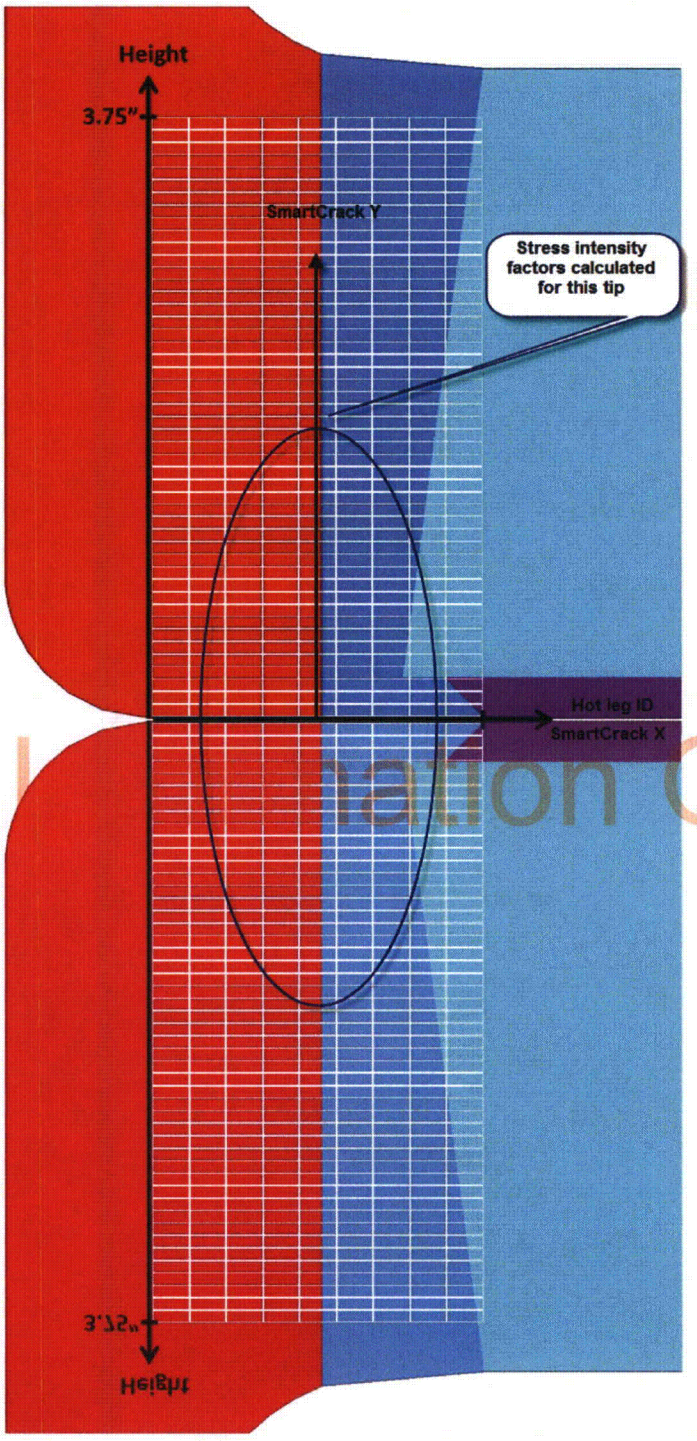

Figure 4: SmartCrack Axial Crack Modeling

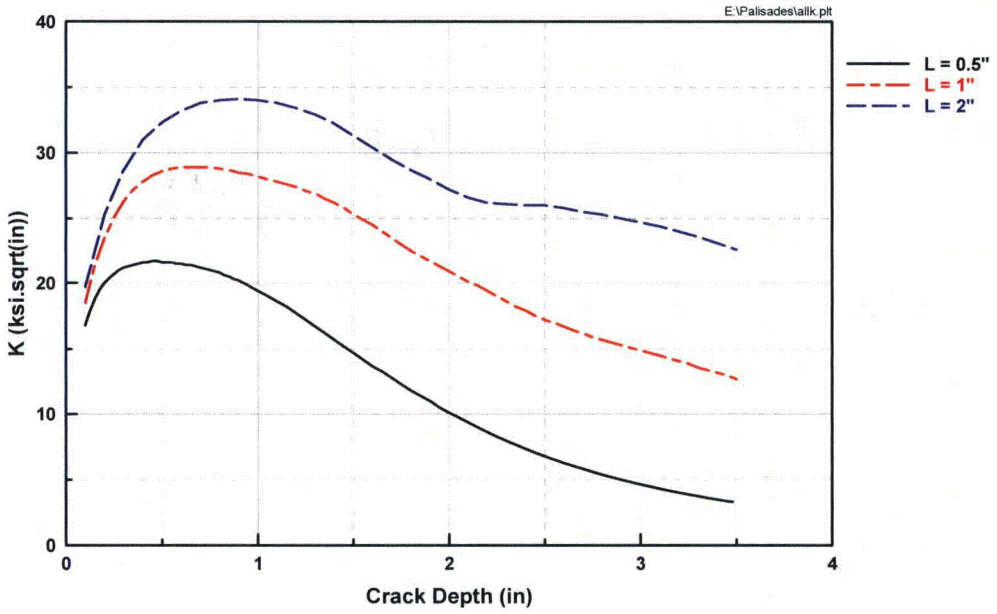

Figure 5: SmartCrack Stress Intensity Factors for Axial Cracks

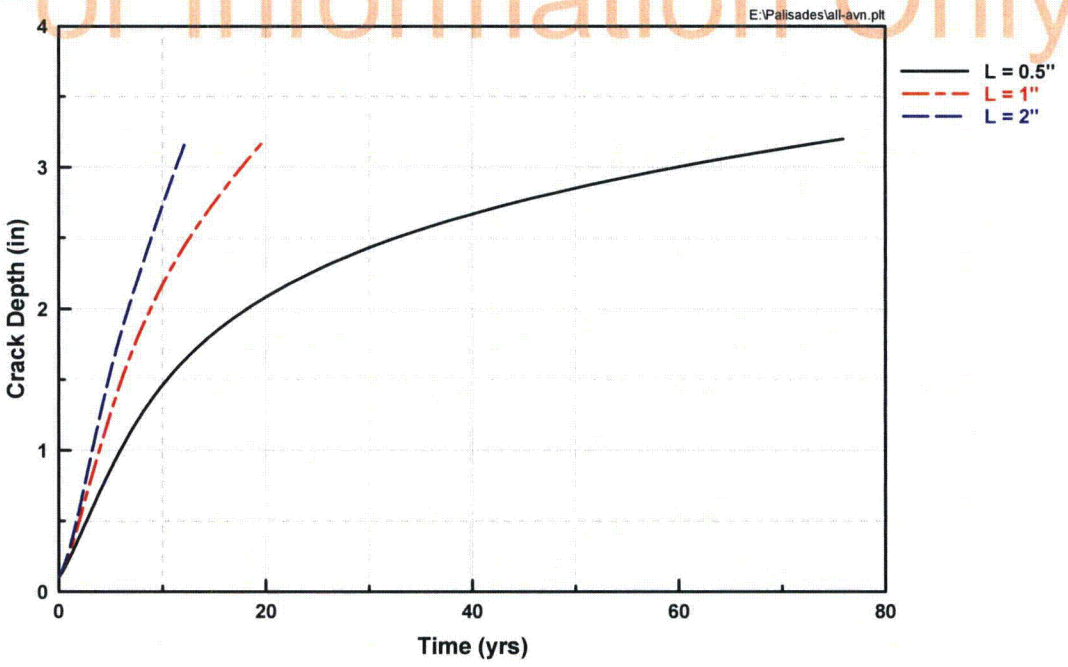

Figure 6: Crack Depth vs. Time for the Growth of Axial Cracks

Structural Integrity Associates, Inc.®

CALCULATION PACKAGE

File No.: 1200895.308

Project No.: 1400148

Quality Program: ☒ Nuclear ☐ Commercial

PROJECT NAME:
Evaluation of Hot Leg Drain Nozzle

CONTRACT NO.:
10404220

CLIENT:	**PLANT:**
Entergy Nuclear	Palisades Nuclear Plant

CALCULATION TITLE:
Hot Leg Drain Nozzle Limit Load Analyses for Flawed Nozzle-to-Hot Leg Weld

Document Revision	Affected Pages	Revision Description	Project Manager Approval Signature & Date	Preparer(s) & Checker(s) Signatures & Date
0	1 - 18 A-1 – A-3	Initial Issue	Gole Mukhim 3/6/14	Richard Bax 3/6/14 Charles Fourcade 3/6/14
1	1 - 23 A-1 - A-3	Reanalyze limit load for revised circumferential crack growth depths.	Chris Lohse 5/8/15	Richard Bax 5/8/15 Wilson Wong 5/8/15

Table of Contents

List of Tables

List of Figures

1.0 OBJECTIVE

The objective of this calculation is to perform a series of ASME Code "Limit Load" evaluations for postulated axial and circumferential flaws for the hot leg drain nozzle at Palisades Nuclear Plant.

Revision 1 incorporates new circumferential crack growth depths that were developed due to an error in an earlier weld residual analysis, which generated an inaccurate residual stress field and resulted in un-conservative crack growth durations.

2.0 METHODOLOGY

Postulated axial and circumferential flaws are defined in a finite element model (FEM) of the hot leg drain nozzle. The flaws originate in the nozzle-to-hot leg dissimilar metal weld (DMW). Operating loads are applied to the FEM and ASME Code "Limit Load" evaluations are performed to determine if the modeled flaw meets the "Limit Load" requirements for continued operation.

2.1 Limit Load Criteria

Per Section III, NB-3228.1 of the ASME Code [1]:

"The limits on General Membrane Stress Intensity (NB-3221.1), Local Membrane Stress Intensity (NB-3221.2), and Primary Membrane Plus Primary Bending Stress Intensity (NB-3221.3) need not be satisfied at a specific location if it can be shown by limit analysis that the specified loadings do not exceed two-thirds of the lower bound collapse load. The yield strength to be used in these calculations is $1.5S_m$."

2.2 Z-Factor of the Nozzle-to-Hot Leg Weld

The nozzle-to-hot leg weld metal is Alloy 82/182 [3, Section 5.0] and is assumed to be applied as a flux type weld. Since flaws will be included in the "Limit Load" evaluations, a load multiplier for ductile flaw extension, or Z-factor, should be included for the weld material. Per Section XI, Appendix C, C-6330 of the ASME Code [2]:

"(a) For austenitic weldments fabricated by shielded metal-arc welds (SMAW) or submerged-arc welds (SAW), the load multiplier is given by:

$$Z = 1.30[1 + 0.010(NPS - 4)]$$

where NPS is the nominal pipe size."

Calculation of the Z-factor is provided in Section 4.0.

3.0 ASSUMPTIONS / DESIGN INPUTS

The FEM of the hot leg drain nozzle for Palisades Nuclear Plant was developed previously in Reference 3. The model was originally developed using the ANSYS, Release 8.1, software package [4]. However, for this evaluation the original model input files (see Appendix A) were rerun using the ANSYS, Release 14.5, software package [5] (the finite element model is shown in Figure 1) and all "Limit Load" evaluations will be performed using ANSYS, Releaser 14.5.

Reference 6b (page 8 of 10 of the referenced document) indicates that, for the hot leg, the bounding thermal transient stress of 1.01 ksi is due to Thermal 002, the deadweight stress is 0.096 ksi and the friction stress is 1.056 ksi. Reference 6b (page 10 of 10 of the referenced document) indicates that these stresses are all axial stresses. However, there are no seismic stresses identified in Reference 6b. Therefore, it was assumed that the Operational Basis Earthquake axial stress is equal to five times the deadweight stress or 5 x 0.096 = 0.480 ksi, based on the transmittal to Entergy in Reference 11.

Reference 7 tabulates the bounding nozzle loads for the hot leg drain nozzle, which are reproduced in Table 1 of this calculation.

Reference 6a (page 1 of 6 of the referenced document) indicates that the nozzle maximum operating pressure and mean temperature occurs during the Safety Valve Operation, during which the pressure is 2650 psi and the mean temperature is 598°F.

4.0 FINITE ELEMENT MODEL

As indicated earlier in Section 3.0, the FEM was previously developed in Reference 3. Three global changes are made to the FEM for the "Limit Load Analysis."

The first change to the FEM is to remove the bottom portion of the hot leg drain nozzle where the nozzle connects to the hot leg drain piping. The region of the nozzle removed reached up to the thicker body of the nozzle (see Figure 1). The purpose in removing the lower portion of the nozzle is to guarantee that the flaw region will be limiting rather than the much thinner nozzle-to-drain piping weld location.

The second change to the FEM is the revision of the material properties to support the "Limit Load" analysis. All of the properties have been replaced with minimum elastic properties and the elastic-perfectly plastic material properties. The elastic properties are as shown in Table 2 and are based on Reference 8 for a conservative temperature of 600°F (normal operating temperature is 593°F [10]).

Per Section 2.1 the yield strength for the elastic-perfectly plastic material curves are based on the $1.5S_m$. The values for the design stress intensity, S_m, are again based on Reference 8 for a temperature of 600°F. For the Alloy 182, nozzle-to-hot leg weld metal, the yield strength of $1.5S_m$ will be reduced by the Z-factor defined in Section 2.2. For this evaluation, the NPS value is defined as the diameter of the nozzle-to-hot leg weld, as taken from the outside surface toe of the weld, furthest from the nozzle. This

maximizes the Z-factor and conservatively reduces the yield strength of the weld material. The diameter, measured from the finite element model [3], is approximately 8 inches. The Z-factor is then determined to be:

$$Z = 1.30[1 + 0.010(NPS - 4)] = 1.30[1 + 0.010(8-4)] = 1.352$$

Thus the yield strength of the Alloy 182 is now defined as $1.5S_m/1.352 = 1.1095S_m$. The yield strengths of all the materials are shown in Table 3.

The third and final change is only for the circumferential flaw evaluation. Due to the reduced flaw duration, it was necessary to more accurately simulate the drain nozzle loading in order to improve the "Limit Load" results. To that end, two 180° "half models" will be utilized to include the effects of a bounding resultant moment. One model will be based on axial symmetry of the hot leg (Global Cartesian Z-direction) and the other will be based on circumferential symmetry of the hot leg (Global Cartesian X-direction). The resultant drain nozzle moment will be applied in the appropriate direction for the given model. The two models are shown in Figure 2.

4.1 Flaw Modeling

A total of three separate flaw geometries were evaluated. One involved a circumferential flaw in the Alloy 182 nozzle-to-hot leg weld, while the other two involved axial flaws that included the Alloy 182 weld and the Alloy 600 nozzle body.

Circumferential flaw growth projections were performed in Reference 9 from 20 years to 60 years in 10 year increments. These projections are tabulated in Table 4. Note, that Table 4 has flaw depths at 0°, 30°, 60° and 90° circumferential azimuths, based on the original 90° "quarter model" FEM. The 40 year circumferential flaw was selected for evaluation. The flaw depths provided in Table 4 are based on a 90° FEM, so the flaw will be mirrored for the two "half models." The 40 year flaw was simulated by selecting elements originally modeled in the Alloy 182 weld material and deactivating them via the ANSYS EKILL command. The deactivated elements have near-zero stiffness contribution to the structure. The selected flaw elements for the two "half models" are shown in Figure 3.

Two axial flaw depth cases were modeled; a 75% part through-wall flaw and a 100% through-wall flaw. In both cases, the axial flaw includes the Alloy 182 nozzle-to-hot leg weld and a corresponding section of the Alloy 600 nozzle. For the 100% through-wall flaw, the flaw extends an additional 2 inches along the Alloy 600 nozzle. Since the model is a 90° "quarter model," the flaws will be simulated by removing symmetry boundary conditions along both the 0° and 90° symmetry planes, effectively creating two flaws; one axial to the plane of the hot leg and one along the circumferential plane of the hot leg. See Figure 5 for an example of the modified boundary conditions, used to simulate the flaw.

5.0 LOADING

5.1 Hot Leg Piping Interface Loads

The hot leg loads are provided in terms of stress and are conservatively applied as tensile pressure loads to the axial free end of the modeled hot leg. The total load is the combination of Pressure + Deadweight + Friction + Thermal + OBE. The pressure load is based on the maximum pressure of 2650 psi per Section 3.0. The pressure load is determined as follows:

$$P_{end\text{-}cap} = \frac{P \cdot ID^2}{\left(OD^2 - ID^2\right)} = \frac{2650 \cdot 41.626^2}{\left(49.626^2 - 41.626^2\right)} = 6{,}290 \text{ psi} = 6.290 \text{ ksi}$$

where,

$P_{end\text{-}cap}$ = End cap pressure on hot leg free end (psi)
P = Internal pressure (psi)
ID = Inside diameter of hot leg (in) [3, Finite Element Model]
OD = Outside diameter of hot leg (in) [3, Finite Element Model]

Therefore, the final axial tensile pressure applied to the free end of the hot leg is:

$$P + DW + Friction + Thermal + OBE = 6.290 + 0.096 + 1.056 + 1.010 + 5 * 0.096 = 8.932 \text{ ksi}$$

5.2 Drain Nozzle Piping Interface Loads

The hot leg drain nozzle piping loads are provided in terms of forces and moments per Table 1.

5.2.1 Loading for the Axial Flaw Evaluations

For the axial flaw evaluations, these loads will be converted to axial stresses and applied as tensile pressure loads to the axial free end of the modeled hot leg drain nozzle. The decision to use calculated axial stresses is because the original model is a 90° "quarter" model and therefore, cannot be used directly for moment loading. Also, axial flaws are highly resistant to plastic failure under the "Limit Load" criteria and the use of equivalent axial loads, which is conservative in terms of a limit load analysis, as the tensile axial load puts the entire cross section into equal stress resulting in plastic collapse at lower stresses than the combination of tensile and compressive stresses that would result from actual moment loading.

The loads from Table 1 were combined by absolute sum and the axial force (Fy) used to determine the axial stress due to the force and the two moments (Mx and Mz), combined into a resultant moment, Mr, by the square root of the sum of the squares (SRSS) used to determine the axial stress due to the moment.

The stress due to the axial force is calculated as:

$$\sigma_{force} = \frac{F}{A} = \frac{0.404 \cdot 1000}{\pi\left(2.28125^2 - 1.15625^2\right)} = 33.3 \text{ psi} = 0.033 \text{ ksi}$$

where,

σ_{force}	=	Stress on nozzle free end due piping axial force (psi)
F	=	Axial force (kips) due to DW + OBE + Normal Operation (from Table 1, Fy)
A	=	Area of nozzle free end – $\pi(OR^2 - IR^2)$, (in^2)
IR	=	Inside radius of nozzle (in) [3, Finite Element Model]
OR	=	Outside radius of nozzle (in) [3, Finite Element Model]

The stress due to the resultant moment, Mr, is calculated as:

$$\sigma_{moment} = \frac{Mr \cdot OR}{I} = \frac{4}{\pi}\frac{\left(19.905 \cdot 1000\right) \cdot 2.28125}{\left(2.28125^4 - 1.15625^4\right)} = 2285.8 \text{ psi} = 2.286 \text{ ksi}$$

where,

σ_{moment}	=	Stress on nozzle free end due piping moments (psi)
Mr	=	Resultant moment (kips) – Resultant moment for DW + OBE was determined separately from Normal Operation and the two added together (from Table 1).
I	=	Moment of Inertia – $(\pi/4)(OR^4 - IR^4)$ (in^4)
IR	=	Inside radius of nozzle (in) [3, Finite Element Model]
OR	=	Outside radius of nozzle (in) [3, Finite Element Model]

The pressure load is based on the maximum pressure of 2650 psi per Section 3.0. The pressure load is determined as follows:

$$P_{end\text{-}cap} = \frac{P \cdot ID^2}{\left(OD^2 - ID^2\right)} = \frac{2650 \cdot 2.3125^2}{\left(4.5625^2 - 2.3125^2\right)} = 916 \text{ psi} = 0.916 \text{ ksi}$$

where,

$P_{end\text{-}cap}$	=	End cap pressure on nozzle end (psi)
P	=	Internal pressure (psi)
ID	=	Inside diameter of nozzle (in) [3, Finite Element Model]
OD	=	Outside diameter of nozzle (in) [3, Finite Element Model]

Therefore, the final axial tensile pressure applied to the free end of the drain nozzle is:

$P + (DW + OBE + Operation)_{Force} + (DW + OBE + Operation)_{Moment} = 0.916 + 0.033 + 2.286 = 3.235$ ksi

5.2.2 Loading for the Circumferential Flaw Evaluations

Since the circumferential flaw will be more influenced by the nozzle piping loads, these evaluations will specifically model the piping loads. As shown earlier in Section 5.2.1, the axial force is 0.404 kips and the resultant moment is 19.905 in-kips.

The drain nozzle loads will be simulated as a tensile axial force and a single moment in the plane of the "half model." The contribution due to end cap pressure will be included in the axial force application. The pressure load is based on the maximum pressure of 2650 psi per Section 3.0. The pressure load is determined as follows:

$$F_{end\text{-}cap} = P \cdot \pi \cdot \left(\frac{ID}{2}\right)^2 = 2650 \cdot \pi \cdot \left(\frac{2.3125}{2}\right)^2 = 11{,}130 \text{ lbs} = 11.130 \text{ kips}$$

where,

$F_{end\text{-}cap}$ = End cap force on nozzle end (lb)
P = Internal pressure (psi)
ID = Inside diameter of nozzle (in) [3, Finite Element Model]

Therefore, the final axial tensile applied load to the free end of the drain nozzle is:

$$P + (DW + OBE + Operation)_{Force} = 11.130 + 0.404 = 11.534 \text{ kips}$$

Since the analyses will be performed using "half models," with the drain nozzle loads applied along the plane of symmetry, it is necessary to reduce the drain nozzle loads by half. Thus, the applied axial load will be 11.534/2 = 5.767 kips, applied in the Global Cartesian Y-direction.

For the axial model, the resultant moment of 19.905/2 = 9.9525 in-kips will applied about the Global Cartesian X-direction, and for the circumferential model, the resultant moment will applied about the Global Cartesian Z-direction.

5.3 Internal Pressure and Mechanical Boundary Conditions

5.3.1 Axial Flaw Evaluations

An internal pressure of 2.650 ksi was applied to all inside surfaces of the FEM including the crack face. The cap load effects of the pressure on the hot leg and drain nozzle have already been discussed in Sections 5.1 and 5.2.1. An example of the applied pressure, including the axial pressure loads applied to the ends of the lot leg and the drain nozzle (see Sections 5.1 and 5.2.1), for the axial flaw in Figure 4.

Symmetry boundary conditions are applied at the nozzle planes of symmetry and the circumferential free end of the hot leg pipe. The nodes at the free end of the hot leg pipe and the hot leg drain nozzle have their respective axial degrees of freedom coupled to simulate the resistance to moment loading similar to that of the un-modeled remainder of the hot leg piping or drain piping. As explained in Section 4.1, the

axial flaws are simulated by removing boundary conditions at the location of the flaw. An example of the applied mechanical boundary conditions for the axial flaw in Figure 5.

5.3.2 Circumferential Flaw Evaluation

An internal pressure of 2.650 ksi was applied to all inside surfaces of the FEM including the crack face. The cap load effects of the pressure on the hot leg and drain nozzle have already been discussed in Sections 5.1 and 5.2.2.

The drain nozzle piping loads and the pressure cap loads are applied at free end of the modeled drain nozzle by making use of a pilot node to transfer the loading. The TARGE170 target element type from the ANSYS element library [5] is used to create the pilot node. The CONTA175 contact element type [5] is used to create the contact surfaces at the free end of the drain nozzle. The pilot node and surfaces are bonded together so that the load applied to the pilot node is transferred to the free end of the drain nozzle. The applied pressure, including the axial pressure load applied to the end of the hot leg, and forces and moments applied to the drain nozzle (see Sections 5.1 and 5.2.2), for the circumferential flaw are shown in Figures 6 and 7.

Symmetry boundary conditions are applied at the nozzle planes of symmetry and the circumferential free end of the hot leg pipe. The nodes at the free end of the hot leg pipe are coupled in the axial direction to simulate the resistance to moment loading similar to that of the un-modeled remainder of the hot leg piping.

For the circumferential "half model," a line of nodes on the inside surface of one circumferential free end are held in the Global Cartesian X-direction to prevent rigid body motion.

In addition, the pilot node for the circumferential "half model" is fixed in the Global Cartesian Z-direction, while the pilot node for the axial "half model" is fixed in the Global Cartesian X-direction

The applied mechanical boundary conditions for the two models are shown in Figures 8 and 9.

6.0 LIMIT LOAD EVALUATION

As indicated in Section 2.1, the limit load for the structure under evaluation must not exceed two-thirds of the lower bound collapse load. This can be restated as 150% of the operating loads are applied to the structure and if the structure does not plastically collapse (in terms of ANSYS finite element analysis, plastic collapse is equated with numeric instability) then the evaluation meets the acceptance criteria for the limit load evaluation. For all four analyses in this calculation, 200% of the operating load was applied. For the 40 year circumferential flaw, 173.28% of the load was reached before plastic collapse for the axial "half model," and 171.13% of the load was reached before plastic collapse for the circumferential "half model". For the 75% through-wall axial flaw, 198.92% of the load was reached before plastic collapse and for the 100% through-wall axial flaw, 187.35% of the operating load was reach before plastic collapse.

7.0 CONCLUSIONS

For a circumferential flaw based on 40 years of growth as defined in Reference 9 or a 100% through-wall axial flaw, the hot leg, hot leg-to nozzle-weld, and the main nozzle body remain structurally stable using the rules of ASME Code, Section III, NB-3228.1.

8.0 REFERENCES

1. ASME Boiler and Pressure Vessel Code, Section III, *Rules for Construction of Nuclear Facility Components*, 2001 Edition with Addenda through 2003.
2. ASME Boiler and Pressure Vessel Code, Section XI, *Rules for Inservice Inspection of Nuclear Plant Components*, 2001 Edition with Addenda through 2003.
3. Structural Integrity Calculation No. 0801136.311, Rev. 1, "Hot Leg Drain Nozzle Finite Element Model for Welding Residual Stress Estimation."
4. ANSYS, Release 8.1 (w/Service Pack 1), ANSYS, Inc., June 2004.
5. ANSYS Mechanical APDL and PrepPost, Release 14.5 (w/ Service Pack 1), ANSYS, Inc., September 2012.
6. Email from Daniel J. Depuydt (Entergy) to Richard Mattson (SI), "Subject: Palisades Primary Coolant Piping and Hot Leg Drain Stress Information," dated February 19, 2014, with attached files, SI File No. 1200895.218.
    a) Pal Hot leg Drain Nozzle Structural and Fatigue Analysis from CENC-1115.pdf
    b) Pal PCS Piping WT and Thermal Expansion from CENC-1115.pdf
7. Structural Integrity Calculation No. 1000035.311, Rev. 0, "Hot Leg Replacement Drain Nozzle Weld Repair Sizing Calculation."
8. ASME Boiler and Pressure Vessel Code, Section II, Part D, *Material Properties*, 2001 Edition with Addenda through 2003.
9. Structural Integrity Calculation No. 1200895.307, Rev. 1, "Hot Leg Drain Nozzle Crack Growth Analyses."
10. Palisades Document No. EC-LATER, Revision 0, "Design Input Record," SI File No. 0801136.202.
11. Email from Dick Mattson (SI) to William Sims (Entergy), Jamie Gobell (Entergy) and John Broussard (Dominion), "Subject: RE: starting point," with attached file Nozzle3-2.pdf, dated February 20, 2014 at 5:36 AM, SI File No. 1200895.220.

Table 1: Bounding Hot Leg Drain Nozzle Loads

Load Case	Forces, kips			Moments, in-kips		
	Fx	Fy	Fz	Mx	My	Mz
Deadweight	0.002	0.123	0.008	0.006	0.036	0.532
Normal Operation	-0.389	0.099	-0.062	-1.542	-1.332	12.358
OBE	0.225	0.182	0.085	2.940	3.744	6.312

Notes:
1) Loads are from Reference 7, Table 1.
2) F_y is in the axial direction of the nozzle.

Table 2: Material Properties - Elastic

Component	Material	Modulus of Elasticity, E, 10^3 ksi[3]	Poisson's Ratio, ν
Hot Leg	SA-516 Grade 70	26.7	0.3
Hot Leg Cladding	ER308L[1]	25.3	0.3
Nozzle	Alloy 600	28.7	0.29
Nozzle-to-Hot Leg Weld	Alloy 182[2]	28.7	0.29

Notes:
1) ER308L is a weld material designation and a base metal equivalent of Type 304 stainless is used.
2) Alloy 182 is a weld material designation and a base metal equivalent of Alloy 600 is used.
3) Properties are based on Reference 8 for a conservative temperature of 600°F (normal operating temperature is 593°F [10])

Table 3: Material Properties - Limit Load Analyses

Component	Material	Yield Strength Criteria	Design Stress, S_m, ksi[3]	Yield Strength ksi
Hot Leg	SA-516 Grade 70	$1.5S_m$	19.4	29.10
Hot Leg Cladding	ER308L[1]	$1.5S_m$	16.6	24.90
Nozzle	Alloy 600	$1.5S_m$	23.3	34.95
Nozzle-to-Hot Leg Weld	Alloy 182[2]	$1.1095S_m$[4]	23.3	25.85

Notes:
1) ER308L is a weld material designation and a base metal equivalent of Type 304 stainless is used.
2) Alloy 182 is a weld material designation and a base metal equivalent of Alloy 600 is used.
3) Properties are based on Reference 8 for a conservative temperature of 600°F (normal operating temperature is 593°F [10])
4) Yield strength of the weld material reduced by the Z-factor, 1.352, as calculated in Section 4.0.

Table 4: Crack Depths at 20 to 60 years for the Circumferential Cracks

Angular Location (degrees)[1]	Crack Depth (inches)				
	20 years	30 years	40 years	50 years	60 years
0	2.07	2.50	2.83	3.04	3.20
30	2.25	2.78	3.11	3.61	TW
60	2.74	3.51	TW	TW	TW
90	3.05	TW	TW	TW	TW

Note:

1) The 0 degree location is oriented along the axis of the hot leg with the 90 degree location oriented along the hoop direction of the hot leg.

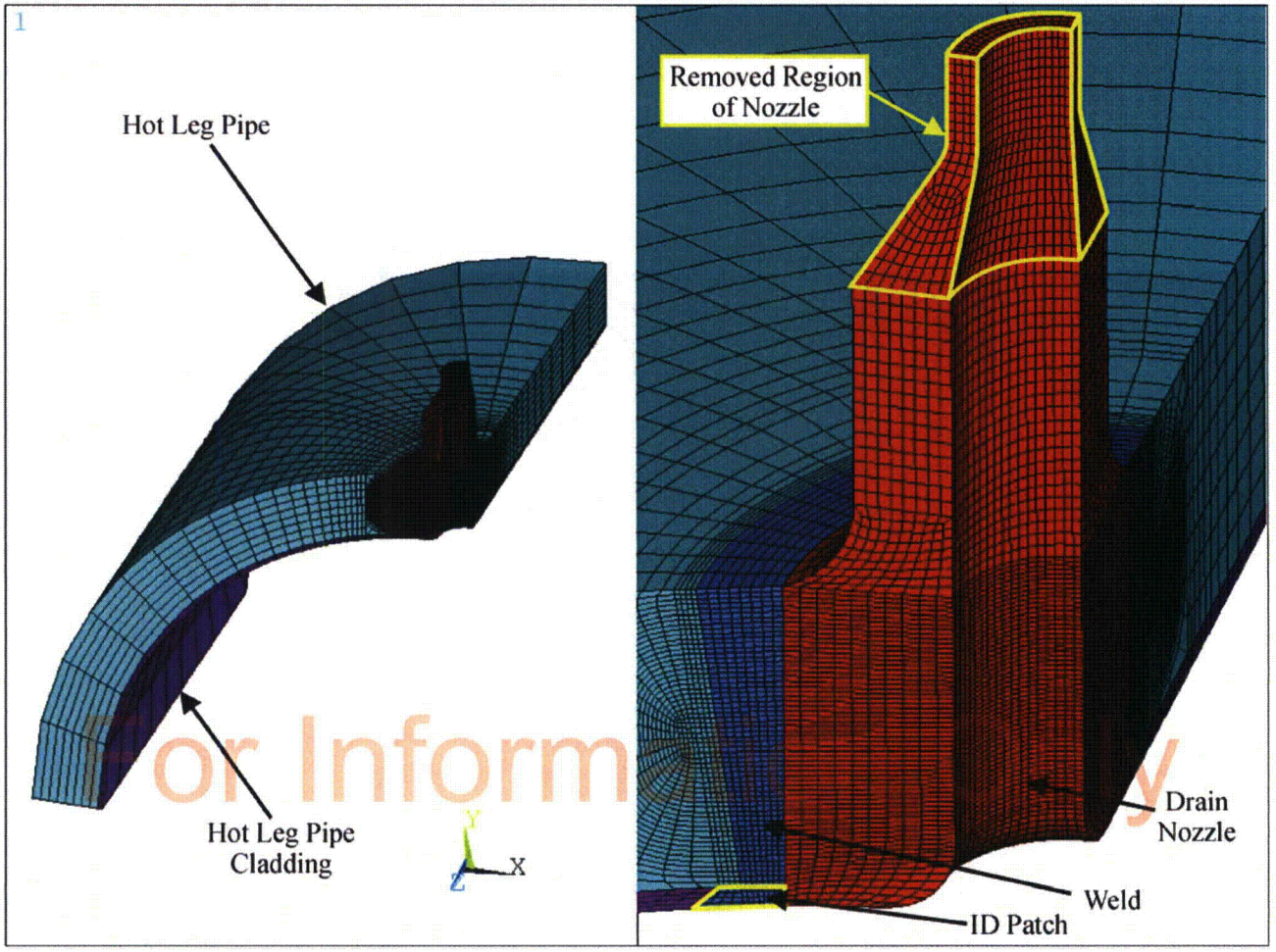

Figure 1: Original Finite Element Model

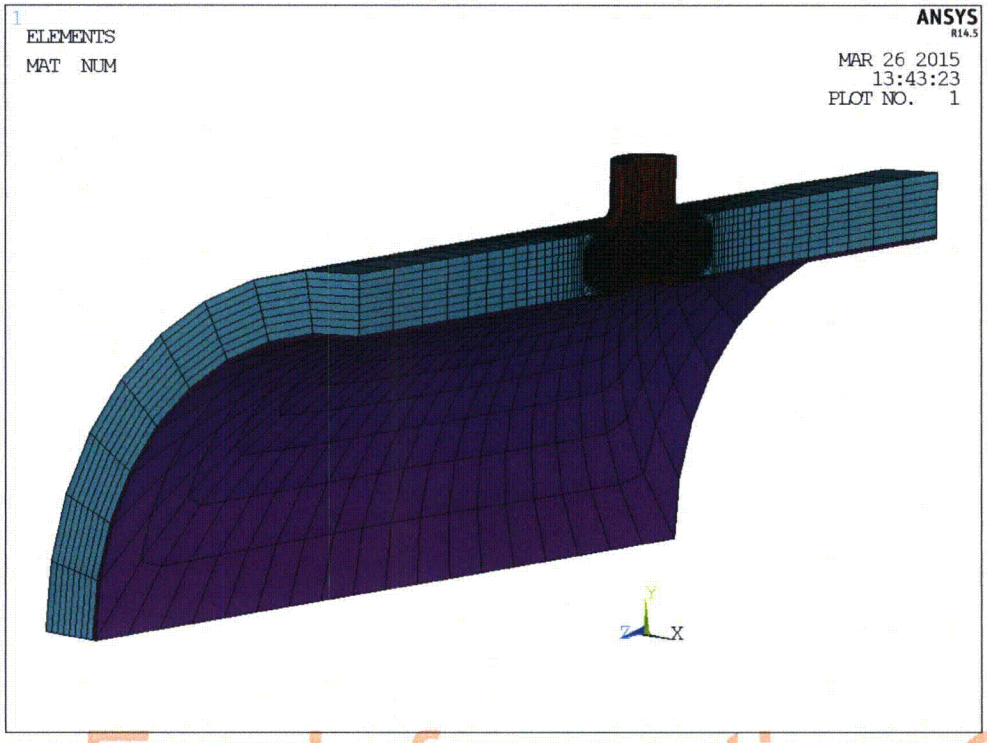

Axial
"Half Model"

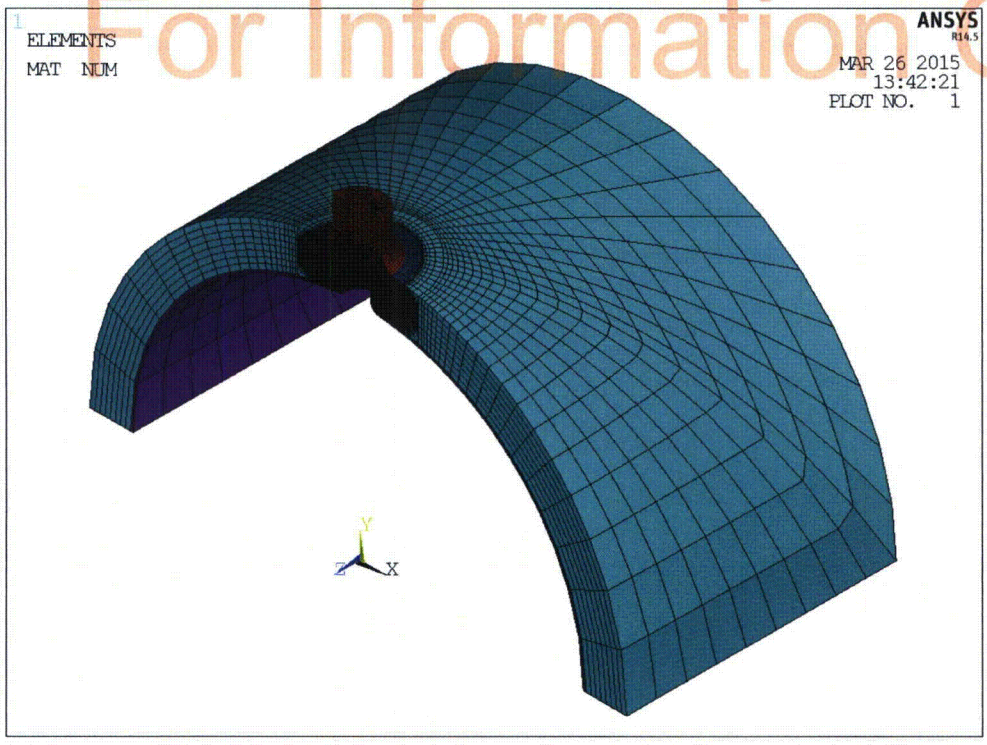

Circumferential
"Half Model"

Figure 2: Finite Element Models for Circumferential Flaw Evaluations

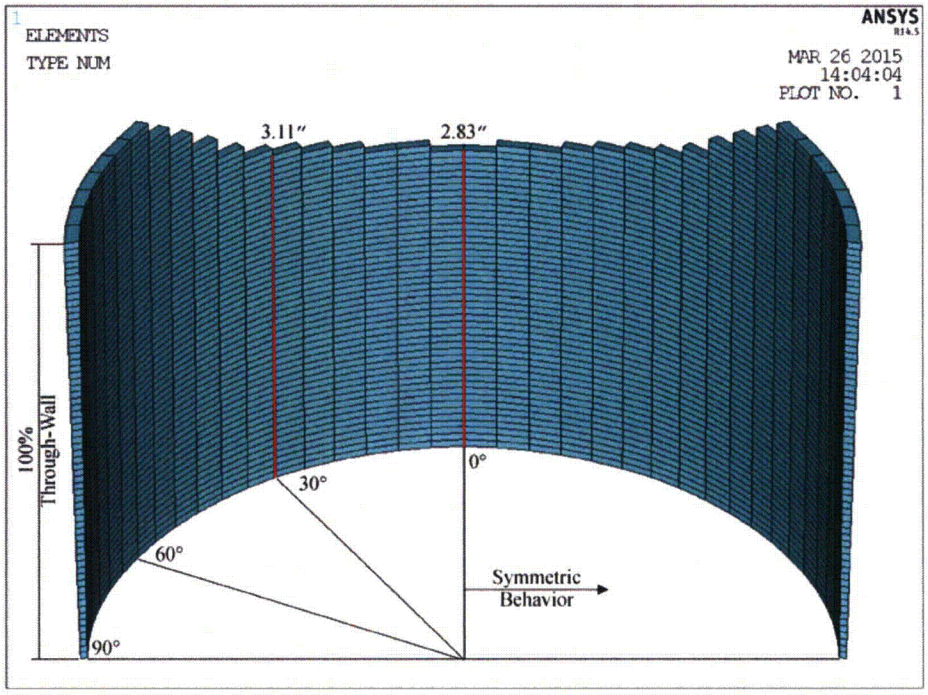

Axial
"Half Model"

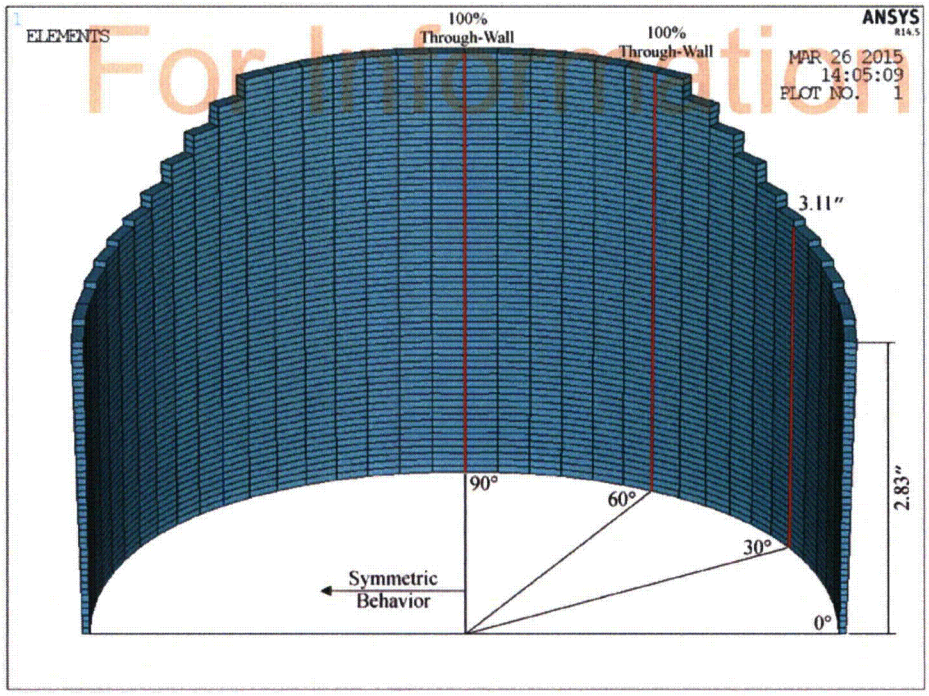

Circumferential
"Half Model"

Figure 3: Flaw Elements that are "Killed" from the Finite Element Models to Create the 40 Year Circumferential Flaw

Note: Flaw is Located at the Nozzle-Weld Interface.

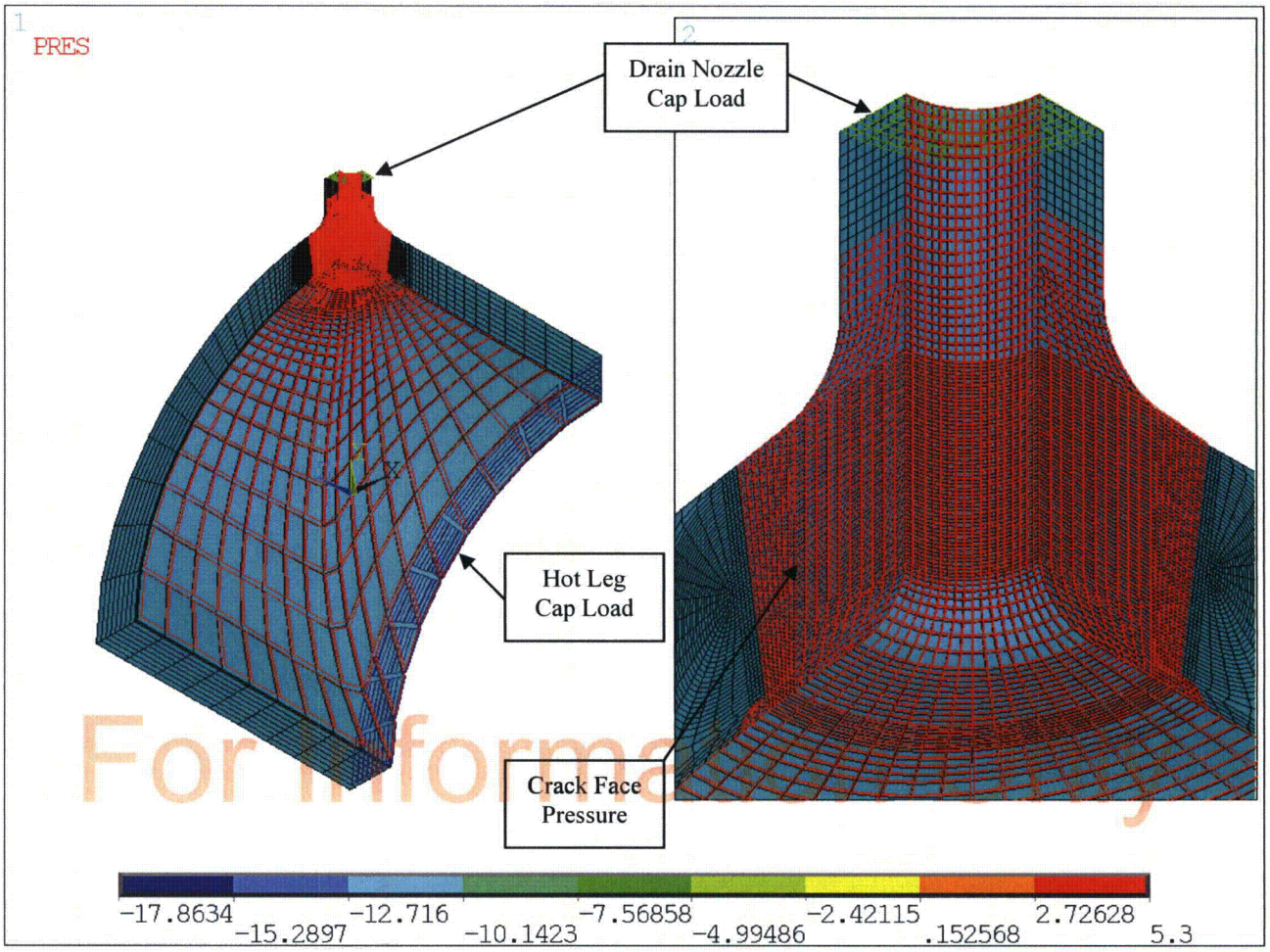

Figure 4: Example of the Applied Pressure Loading for the Finite Element Model for the 100% Through-Wall Axial Flaw

(Note: Units are in terms of ksi)

(Note: The loads shown are at 200% of the operating loads per Section 6.0)

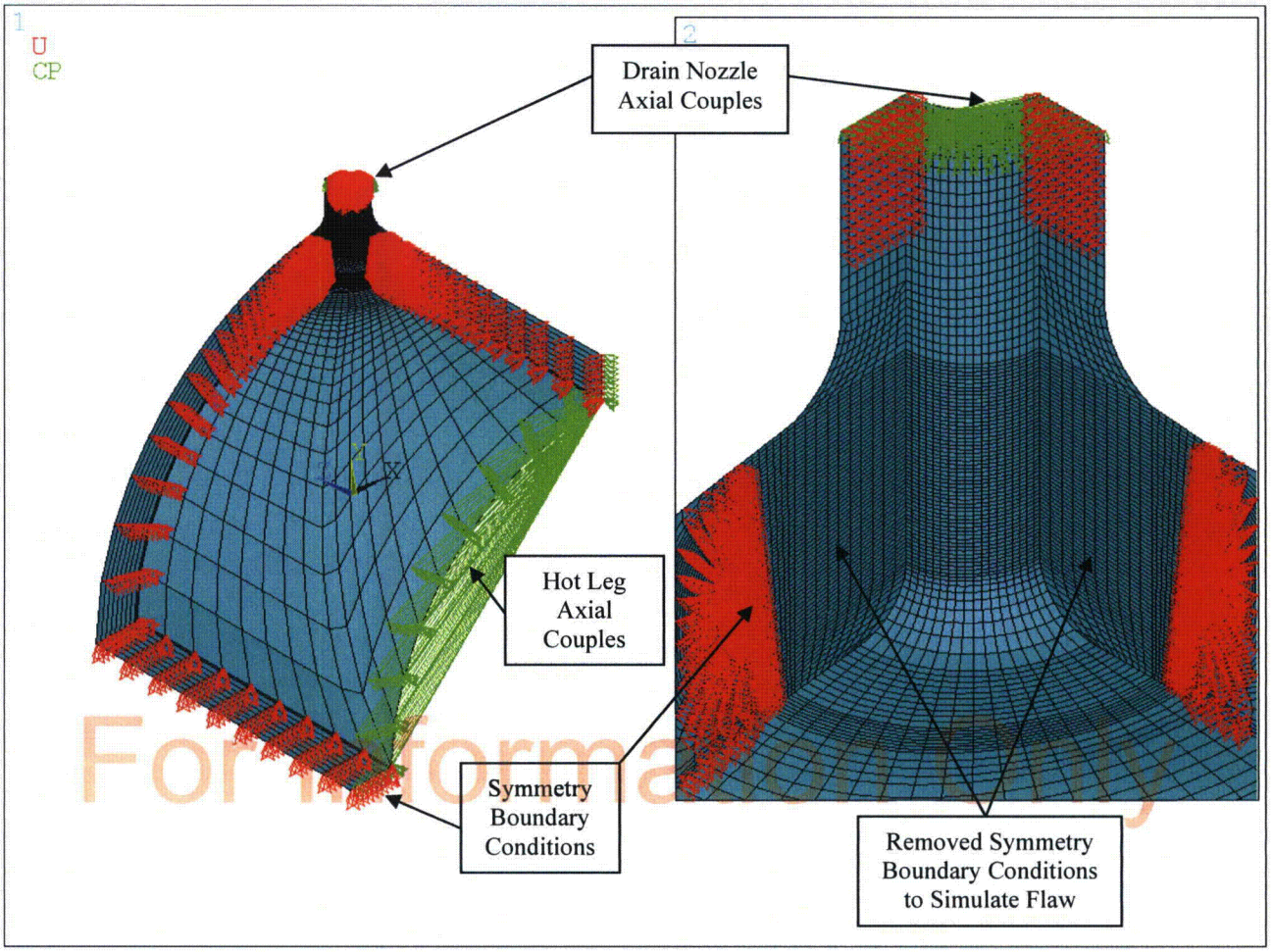

Figure 5: Example of the Applied Mechanical Boundary Conditions for the Finite Element Model to Create the 100% Through-Wall Axial Flaw

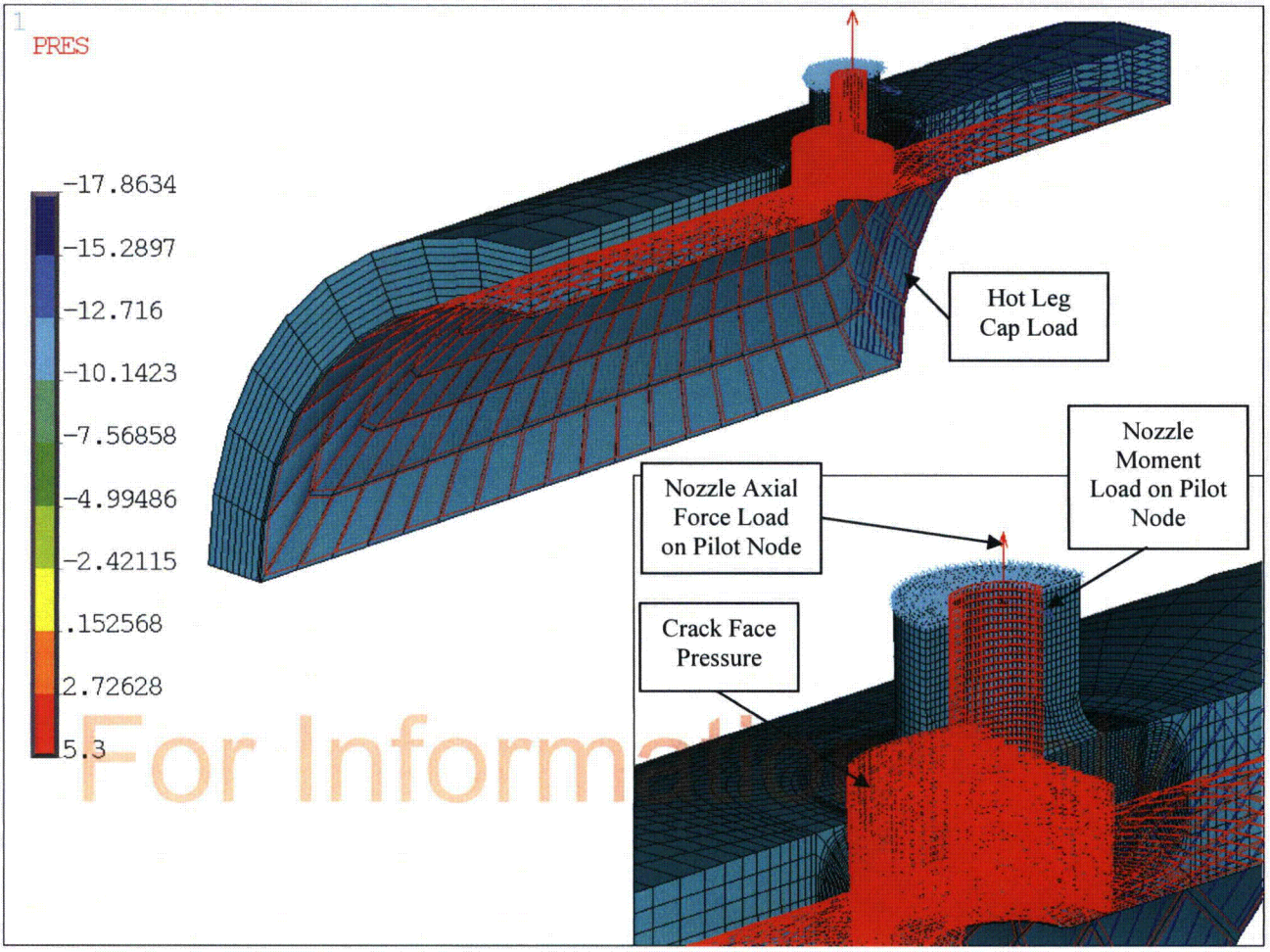

Figure 6: Applied Pressure Loading for the Axial "Half Model" Finite Element Model for the 40 Year Circumferential Flaw

(Note: Units are in terms of ksi)

(Note: The loads shown are at 200% of the operating loads per Section 6.0)

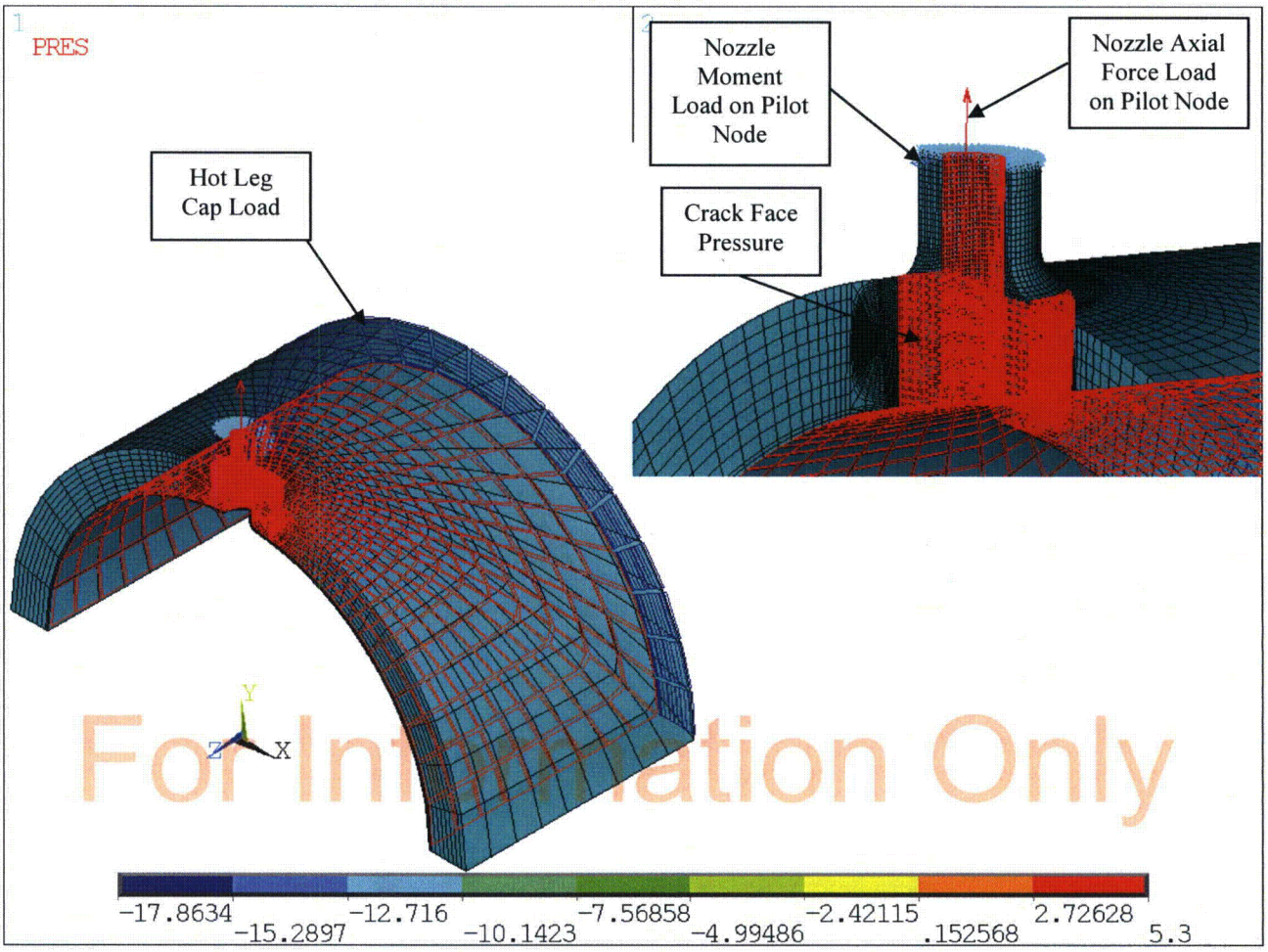

Figure 7: Applied Pressure Loading for the Circumferential "Half Model" Finite Element Model for the 40 Year Circumferential Flaw

(Note: Units are in terms of ksi)

(Note: The loads shown are at 200% of the operating loads per Section 6.0)

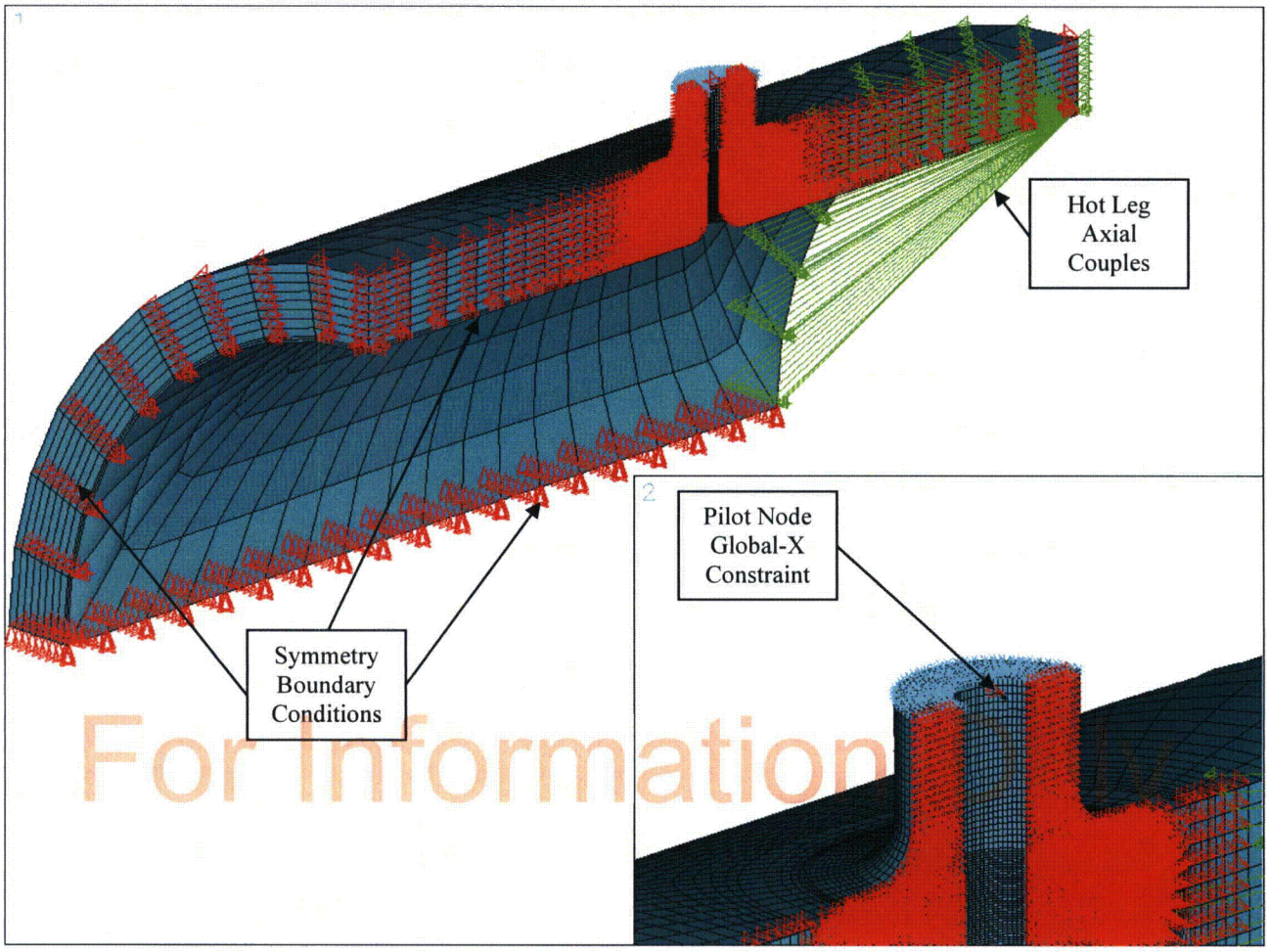

Figure 8: Applied Mechanical Boundary Conditions for the Axial "Half Model" Finite Element Model for the 40 Year Circumferential Flaw

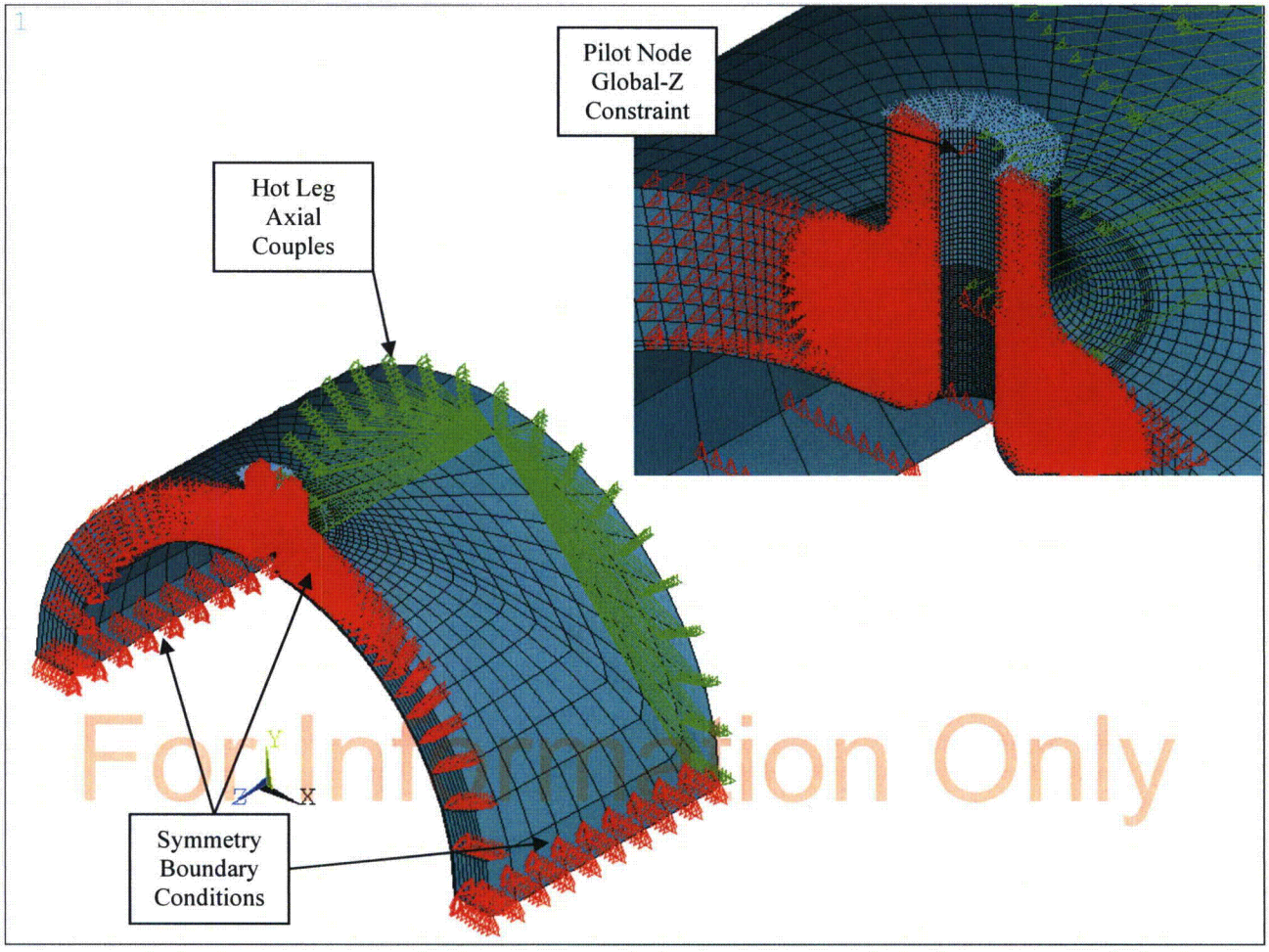

Figure 9: Applied Mechanical Boundary Conditions for the Circumferential "Half Model" Finite Element Model for the 40 Year Circumferential Flaw

APPENDIX A

ANSYS INPUT AND OUTPUT FILES

Files for Creating Basic Geometry from Reference [3]

Geometry Inputs	Description
HL_Drain_MISO.INP	Main geometry input file that uses all the files listed below.
MProp_MISO_PALS.INP	Material property input file (Multilinear isotropic hardening behavior)
Deg90_lines.INP	Sub-Geometry file that is used in the main file - HL_Drain_*.INP
Deg120_lines.INP	Sub-Geometry file that is used in the main file - HL_Drain_*.INP
Deg150_lines.INP	Sub-Geometry file that is used in the main file - HL_Drain_*.INP
Deg180_lines.INP	Sub-Geometry file that is used in the main file - HL_Drain_*.INP
first30vol.INP	Sub-Geometry file that is used in the main file - HL_Drain_*.INP
second30vol.INP	Sub-Geometry file that is used in the main file - HL_Drain_*.INP
third30vol.INP	Sub-Geometry file that is used in the main file - HL_Drain_*.INP
IDpatch_volmesh.INP	Sub-Geometry file that is used in the main file - HL_Drain_*.INP
weldmesh.INP	Sub-Geometry file that is used in the main file - HL_Drain_*.INP
IDpatch_fix.INP	Sub-Geometry file that is used in the main file - HL_Drain_*.INP
butterlike_volmesh.INP	Sub-Geometry file that is used in the main file - HL_Drain_*.INP
cladnextto_IDpatch.INP	Sub-Geometry file that is used in the main file - HL_Drain_*.INP
volnextto_butterlike.INP	Sub-Geometry file that is used in the main file - HL_Drain_*.INP
boss.INP	Sub-Geometry file that is used in the main file - HL_Drain_*.INP
pipeandclad.INP	Sub-Geometry file that is used in the main file - HL_Drain_*.INP
HL_Drain_COMPONENTS1.INP	Sub-Geometry file that is used in the main file - HL_Drain_*.INP
clearfornewscheme.INP	Sub-Geometry file that is used in the main file - HL_Drain_*.INP
autoweld.INP	Sub-Geometry file that is used in the main file - HL_Drain_*.INP
movetheboss.INP	Sub-Geometry file that is used in the main file - HL_Drain_*.INP
selection.INP	Sub-Geometry file that is used in the main file - HL_Drain_*.INP
newnugidpatch.INP	Sub-Geometry file that is used in the main file - HL_Drain_*.INP
selbutter.INP	Sub-Geometry file that is used in the main file - HL_Drain_*.INP
workontheboss.INP	Sub-Geometry file that is used in the main file - HL_Drain_*.INP
newpipeandcladparts.INP	Sub-Geometry file that is used in the main file - HL_Drain_*.INP
HL_Drain_COMPONENTS2.INP	Sub-Geometry file that is used in the main file - HL_Drain_*.INP

Files for Limit Load Analysis

File Name	Description
HL_Drain_MISO.db	ANSYS database file created by file listed in previous table, which is the base file from which all flaws and loading are applied.
piping load stresses.xls	Excel spreadsheet to calculate the hot leg drain nozzle loads.
Limit_40_1.inp	ANSYS Input file to create a circumferential "half model," with a 40 year circumferential flaw, apply 200% of operating load and perform elastic-perfectly plastic analysis.
Limit_40_1.mntr	ANSYS output file for a circumferential "half model," with a 40 year circumferential flaw that documents time history of results. Note that the total time represents the percentage of applied load.
Limit_40_2.inp	ANSYS Input file to create an axial "half model," with a 40 year circumferential flaw, apply 200% of operating load and perform elastic-perfectly plastic analysis.
Limit_40_2.mntr	ANSYS output file for an axial "half model," with a 40 year circumferential flaw that documents time history of results. Note that the total time represents the percentage of applied load.
Limit_AXL_75.inp	ANSYS Input file to create 75% through-wall axial flaw, apply 200% of operating load and perform elastic-perfectly plastic analysis.
Limit_AXL_75.mntr	ANSYS output file for 75% through-wall axial flaw that documents time history of results. Note that the total time represents the percentage of applied load.
Limit_AXL_100_2.inp	ANSYS Input file to create 100% through-wall axial flaw, apply 200% of operating load and perform elastic-perfectly plastic analysis.
Limit_AXL_100_2.mntr	ANSYS output file for 100% through-wall axial flaw that documents time history of results. Note that the total time represents the percentage of applied load.